

Proton Capture into the Giant Dipole Resonance of $^{40}\text{Ca}^\dagger$

E. M. Diener,* J. F. Amann, and P. Paul†

Department of Physics, State University of New York, Stony Brook, New York

(Received 28 February 1972)

The $^{39}\text{K}(p,\gamma)^{40}\text{Ca}$ reaction has been studied from 6.5- to 17-MeV bombarding energy covering the electric giant dipole resonance (GDR) in ^{40}Ca . The GDR displays fine, intermediate, and gross structure. A fluctuation analysis of the fine structure gives a coherence width ~ 25 keV and indicates that compound levels contribute $<3\%$ to the total dipole strength. The intermediate structure has widths clustered between 150 and 450 keV. Despite the large yield fluctuations angular distributions have a uniform shape throughout the GDR with $A_2 = -0.33$, characteristic of dominating f -wave capture. A broad coherent state observed at 19.3 MeV contains 90% of the capture strength with the remainder contained in a weak broad peak at 22 MeV. These positions and relative strengths agree well with calculations of the coherent dipole states based on 1p-1h excitations. However, continuum calculations fail to predict the total widths and angular distributions.

I. INTRODUCTION

Radiative proton capture has proved an important reaction for studies of the electric giant dipole resonance (GDR) since it relates very directly to the particle-hole structure of the involved states. The many nuclei in the p and s, d shells have been studied experimentally through proton capture showing both the successes and the limitations of the microscopic 1p-1h model. Typically, the calculations done with realistic forces for the residual interaction, and often coupled to the continuum by the formalism of Buck and Hill,¹ yield fewer dipole resonances than are observed and fail to reproduce the uniformity of the proton angular distributions found throughout the GDR region even when the resonance appears broken up into many peaks. The GDR of ^{16}O is an extensively studied case where five resonances are observed rather than the two predicted by the simple 1p-1h model.² The additional structure is usually ascribed to admixtures of 2p-2h or 3p-3h states. It is, however, of interest to find a case where the predictions of the basic model can be checked without additional complication. ^{40}Ca appears as the appropriate choice for such a study because it has a very simple ground state and thus a predictable GDR. On the other hand, it has such a dense spectrum of excited states that their influence on the collective state may be statistical.

The electric dipole states of ^{40}Ca have recently been calculated by Blomquist and Kuo³ in a 1p-1h bound-state formalism with realistic forces, and by Marangoni and Saruis⁴ in the coupled-channel formalism. Both of these, and some earlier calculations, concentrate more than 80% of the dipole strength in a single state near 19 MeV excitation.

Previous experimental data over the GDR energy region in ^{40}Ca were reported for the $^{39}\text{K}(p,\gamma)^{40}\text{Ca}$ reaction by Hafele, Bingham, and Allen⁵ with ~ 100 -keV resolution and in the photoneuclear reactions $^{40}\text{Ca}(\gamma, n_0)$ and (γ, p_0) by Wu *et al.*⁶ with ~ 50 -keV resolution. Both results indicate considerable structure in the GDR of ^{40}Ca .

The present paper gives new results on the GDR region of ^{40}Ca as observed in the proton-capture reaction. Making use of the high efficiency of the Stony Brook NaI γ detector, the excitation function was obtained with ~ 30 -keV energy resolution which is of the order of the expected coherence width of background compound states in ^{40}Ca . Thus, an analysis could be made of the fine and intermediate structure in a statistical approach. It will be shown that the gross structure extracted from the data is in good agreement with the theoretical predictions of the 1p-1h model. Angular distributions were also obtained and are not fully in accordance with the coupled-channel calculations.

II. EXPERIMENTAL PROCEDURE

Thin targets of ^{39}K were bombarded by protons with energies between 4 and 17.5 MeV from the Stony Brook tandem accelerator. Deexcitation γ rays leading to the ground and first few excited states were detected in a large NaI detector with anticoincidence shield.⁷ ^{39}K targets were prepared by evaporation of natural potassium metal under vacuum *in situ* onto $20\text{-}\mu\text{g}/\text{cm}^2$ carbon foils, with thicknesses ranging from 20 to 50 keV as determined from the profile of the 4.903-MeV resonance observed in the $^{39}\text{K}(p,\gamma)^{40}\text{Ca}$ reaction.⁸

Two typical γ spectra obtained are presented in Fig. 1. The left spectrum measured at a bom-

bombarding energy of 10.143 MeV shows the performance of the detector to the γ radiation and the neutron background. As indicated, the γ_0 transition is the outstanding peak with a resolution of $\sim 5\%$ at $E_\gamma = 18$ MeV. The very large background radiation at energies below 10 MeV is cut off by an electronic threshold. The residual counts below the γ_0 peak are probably due to transitions to ^{40}Ca excited states, while the counts just above the γ_0 peak occur at the energy of the γ_0 transition in ^{42}Ca , which results from capture by the 6.88% ^{41}K component present in the target. To indicate that the γ spectrum is not so clean at all bombarding energies, the right-hand side of Fig. 1 shows a spectrum taken at 14.312 MeV. In addition to a γ_0 peak, transitions to the lowest excited states around 4 MeV are now observed. Attempts to extract the various final states were not successful. However, the γ_0 transition is still well separated, and in all spectra the strength of this peak was simply obtained by integrating over the indicated interval.

Absolute cross sections were obtained from the γ yield by direct calculation, which requires knowledge of target thickness, total charge which entered the target, the solid angle subtended by the detector, and the efficiency of the detector. The latter consists of the intrinsic efficiency of the collimated NaI crystal which was taken as 100% (after correction for absorption in materials between the target and crystal) and the electronic rejection ratio. This ratio could be obtained for each run from the accepted and rejected spectra, stored separately in a pulse-height analyzer. The

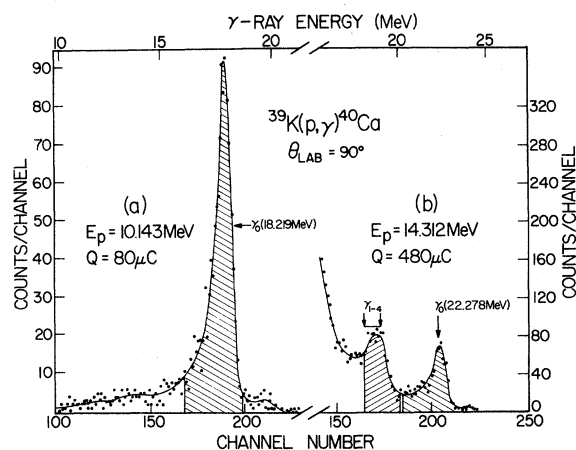


FIG. 1. High-energy portion of the γ spectrum observed at 90° in the $^{39}\text{K}(p, \gamma)^{40}\text{Ca}$ reaction. Transitions to the ground state (γ_0) and the first four excited states are indicated. The shaded intervals were used for yield determination (see text).

calculation yielded the number 0.029 sr for the product of solid angle and efficiency for the geometry used in the runs at 90° . A check on this calculation was made by a comparison with the known absolute thick-target yield⁹ of the $^{12}\text{C}(p, \gamma_0)^{13}\text{N}$ reaction from the first $T = \frac{3}{2}$ resonance at $E_p = 14.231$ MeV, and agreement was obtained within 3%.

III. RESULTS FOR THE GROUND-STATE TRANSITION

The excitation function for the ground-state transition measured at 90° with respect to the beam direction is given in Fig. 2. The data were obtained in 30-keV steps from 6.5- to 15.0-MeV bombarding energy, and in 100-keV steps from 15.0 to 17.5 MeV. Target thickness was 30-keV to 11.0-MeV protons. The excitation curve shows clearly the ~ 3 -MeV-wide peak associated with the GDR centered at $E_p \sim 11$ MeV. The maximum cross section of $8.9 \mu\text{b}/\text{sr}$ ($\pm 30\%$) is attained at $E_p = 10.65$ MeV, corresponding to an excitation energy of 18.7 MeV. The absolute cross sections reported previously by Hafele, Bingham, and Allen⁵ for this reaction agree with the present curves when averaged over 100 keV to match Hafele's energy resolution. Wu *et al.*⁶ obtained results from the photoproton reaction $^{40}\text{Ca}(\gamma, p_0)^{39}\text{K}$ which systematically exceeded by about 15% the upper limits on the inverse-reaction cross sections derived from the present work.

Superimposed on the GDR envelope are peaks of intermediate width $\Gamma \approx 150$ to 400 keV, and fine structure ≤ 50 keV wide. This fine structure persists in the region below the GDR although with reduced amplitude. This hierarchy of gross, intermediate, and fine structure has been observed before in other nearby nuclei, notably¹⁰ ^{28}Si , but ^{40}Ca is a particularly beautiful example because it shows clearly only a single broad envelope rather than the several broad components present in ^{28}Si .

Several additional investigations were made into the characteristics of the fine structure. In order to determine the smallest width of the fine structure, the segment of the excitation function between 11.315 and 11.515 MeV was examined in small steps with a target only 2 keV thick to 11-MeV protons. The resulting yield curve shown in the inset of Fig. 2 indicates that the finest observed width is ~ 25 keV wide. This observed width is quite in agreement with the result from a fine structure analysis of the $^{39}\text{K}(p, \alpha)$ reaction¹¹ over the bombarding energy range 10 and 13 MeV, which gave a coherence width between 10 and 30 keV. To study the dependence of fine and intermediate structure on the detection angle, the detector was moved to 45° and the excitation function repeated in the energy range from 10.92 to 11.64

MeV with a target 20 keV thick to 11.0-MeV protons. The yield curve is compared in Fig. 3 with the corresponding section of the 90° yield curve. The two curves are very similar except that the peaks in the 45° curve are sharper, presumably, because a thinner target was used for the latter. Hence, it is anticipated that angular distributions will not change rapidly with excitation energy despite the considerable amount of structure present in the excitation function. This feature has been observed in other nuclei, with ^{28}Si again being an excellent example.

Angular distributions were measured at the bombarding energies indicated by arrows in Fig. 2. Each distribution was fitted with a sum of Legendre polynomials $W(\theta) = 1 + \sum A_i P_i(\cos\theta)$, with $i=1$ to 4, and the resulting coefficients are plotted in Fig. 4 against excitation energy. A_2 is negative and large throughout the GDR region, with an average value of $A_2 = -0.33$ being within the errors at most points. The only significant deviation in the GDR

occurs at $E_p = 10.63$ MeV where $A_2 = -0.55 \pm 0.10$. This energy coincides with a strong intermediate structure peak; however, there is no general correlation between intermediate structure and deviations of the A_2 coefficients from the average. The uniformity of the angular distributions throughout the GDR is contrasted by the result obtained at the peak at $E_p = 5.8$ MeV, significantly below the GDR. Here the angular distribution is forward peaked with $A_2 = +0.60$. In a simple one-configuration description of the dipole states, this sign change amounts to a switch from a non-spin-flip transition in the GDR to a spin-flip transition at the 5.8-MeV peak. The A_3 and A_4 coefficients vanish within the errors at all energies, attesting to the predominantly dipole character of the γ transition. At several excitation energies around 20 MeV a non-vanishing A_1 coefficient indicates interference with $M1$ or $E2$ radiation, probably the effect of the giant quadrupole resonance.

Based on the average angular distribution, the

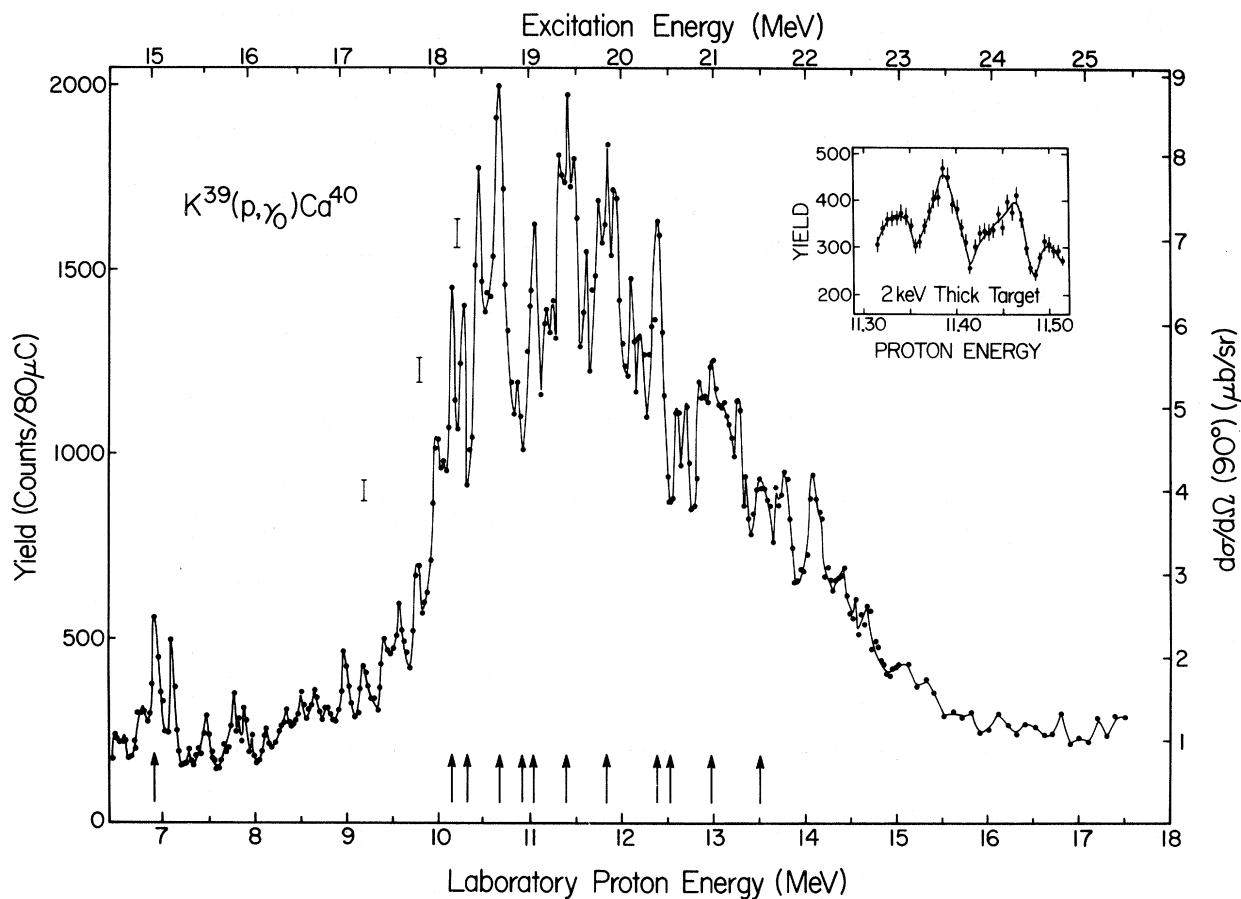


FIG. 2. Excitation function (mostly in 20-keV steps) of the γ_0 yield at 90° over the GDR regions of ^{40}Ca . Complete angular distributions were taken at energies indicated by arrows. The insert shows the portion from 11.30 to 11.56 MeV taken in 2-keV steps.

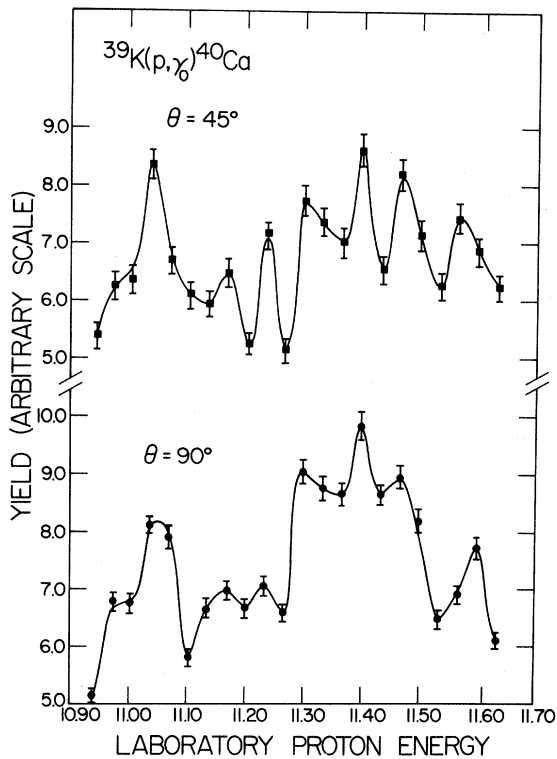


FIG. 3. Comparison of the γ_0 yield function observed at 45° (top) and 90° (bottom) over a segment of the GDR in ^{40}Ca .

yield curve in the region from 14.67- to 25.39-MeV excitation energy gives an integrated cross section of 77 MeV mb or 13% of the classical dipole sum rule. The total γ -absorption cross section in ^{40}Ca integrated up to 25 MeV exhausts $\sim 65\%$ of the sum rule,¹² with less than $\frac{1}{5}$ of this appearing in the neutron channel.¹³ On the assumption that only single-neutron and single-proton resonant emission contributes to the decay of the GDR up to 25 MeV [the (γ, np) threshold occurs at 21.42 MeV], the present results then imply that approximately $\frac{1}{4}$ of the photoproton strength goes to the ground state of ^{39}K . This ratio is quite plausible as can be seen from a comparison of the strengths of the two most important particle-hole components in the GDR, namely $C_1 = (1f_{5/2})(1d_{3/2})^{-1}$ and $C_2 = (1f_{7/2})(1d_{5/2})^{-1}$, of which only the first connects strongly to the ground state of ^{39}K . The 1p-1h wave function³ for the GDR gives the ratio $C_1^2 / (C_1^2 + C_2^2) \approx \frac{1}{3}$. The additional effect of the $2p_{3/2}$ excitations will reduce this ratio.

Averaging the yield curve of Fig. 2 over sliding energy intervals of various arbitrary widths gives the set of excitation functions of Fig. 5. These curves can now be compared to earlier measurements made with poorer energy resolution.^{5, 6, 14} The data averaged over 100 keV exhibit 12 "intermediate" peaks between 18 and 22 MeV with widths

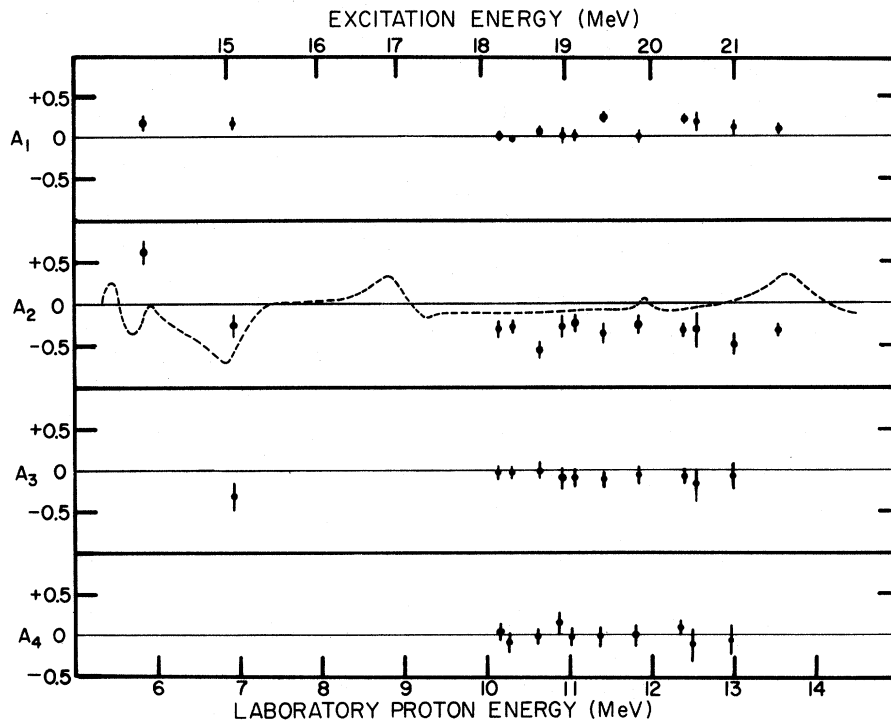


FIG. 4. Plot of Legendre polynomial coefficients A_1 to A_4 determined from $^{39}\text{K}(p, \gamma)^{40}\text{Ca}$ angular distribution as a function of bombarding energy. The dashed curve results from the coupled-channel calculation of Ref. 4.

ranging from 150 to 450 keV and located at energies in Table I. Corresponding peaks apparent in the earlier data of Hafele, Bingham, and Allen,⁵ obtained with 100-keV resolution, and in the work of Wu *et al.*⁶ for the inverse (γ, p_0) reaction, obtained with 50-keV resolution, are included for comparison. All data correlate in the structure and, in addition, Wu has observed⁶ strong correlations between structure in the (γ, p_0) and (γ, n_0) reactions. This will be further discussed below. The gross structure obtained with the 1.5-MeV averaging interval indicates a dominant wide peak around 19 MeV, and a smaller one on the high-energy side. After conversion of this curve to obtain the (γ, p_0) excitation function, it was fitted with two peaks, each having the energy dependence¹⁵

$$\sigma(E) = \frac{\sigma_0}{1 + (E^2 - E_0^2)^2 / (\Gamma E)^2} \quad (1)$$

This gives the resonance parameters listed in Table II and puts the energy of the dominant state at 19.3 ± 0.1 MeV.

IV. FLUCTUATION ANALYSIS OF ^{40}Ca FINE STRUCTURE

In the case of a reaction which occurs at excitation energies where the compound-nucleus levels overlap, Ericson¹⁶ has shown that fine structure can be expected from coherent interference among overlapping levels of the same total angular momentum J and parity π . The reaction amplitudes of these levels are assumed to have random phases and all compound-nucleus levels of given J are taken to have equal total width. The latter assumption is justified by the argument that, at high excitation energies, many partial widths contribute to the total width but no partial width dominates. The total width and the average energy spacing of the

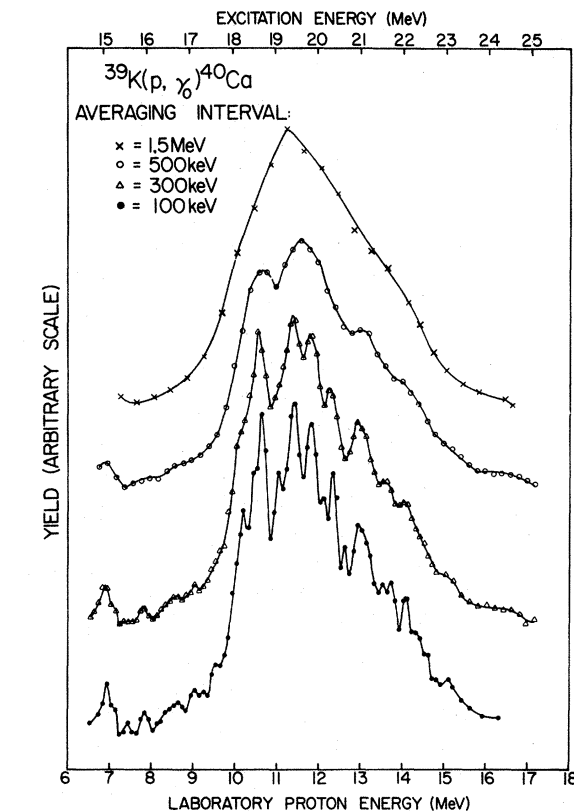


FIG. 5. The γ_0 excitation of Fig. 2 averaged over various sliding energy intervals of widths between 100 keV and 1.5 MeV, to display the intermediate and gross structure in the GDR.

coherently interfering levels are denoted here by Γ and D , respectively. Whereas Ericson assumed that the condition $(\Gamma/D) \gg 1$ must be satisfied for his theory to be applicable, Moldauer¹⁷ has shown that $(\Gamma/D) \geq 1$ is sufficient. The theory then pre-

TABLE I. Excitation energies (in MeV) of intermediate structure peaks observed in ^{40}Ca .

Present work	$^{39}\text{K}(p, \gamma_0)^{40}\text{Ca}$ Hafele, Bingham, and Allen (Ref. 5)	$^{40}\text{Ca}(\gamma, p_0)^{39}\text{K}$ Wu <i>et al.</i> (Ref. 6)
18.26	18.2	18.20
18.68	18.7	18.70
19.07	19.0	19.05
19.45	19.4	19.35
		19.60
19.85	19.8	19.90
20.13 (weak)		
20.43	20.3	20.35
20.65		20.55
20.94 (broad)	21.0	21.20
21.49		
21.69		21.80
22.06	22.0	

dicts fine structure correlated in energy over a range $\approx \Gamma$ termed the coherence width.

In the present case of the $^{39}\text{K}(p, \gamma_0)^{40}\text{Ca}$ reaction, it was deduced from the angular distributions that the γ_0 transition is predominantly $E1$ in character at all energies above $E_x \approx 16$ MeV. Since the well-known isospin selection rules prohibit $\Delta T = 0$ $E1$ transitions in self-conjugate nuclei, only compound levels with $J^\pi = 1^-$, $T = 1$ are considered below. It will be shown that, for these levels, the condition $(\Gamma/D) \geq 1$ is satisfied in the GDR region in ^{40}Ca . This conclusion remains true if isospin is not a good quantum number for the compound levels since D would then be even smaller.

From the data obtained with the 2-keV-thick target (see the inset of Fig. 2), it is concluded that $\Gamma \approx 25$ keV at $E_x = 19$ MeV. Noting that the $T = 1$ levels in ^{40}Ca are isobaric analogs of levels in ^{40}K , D can be estimated from the spacing of isolated resonances observed in the $^{39}\text{K}(n, \gamma)^{40}\text{K}$ reaction at neutron energies below 300 keV, and then extrapolated to 19 MeV excitation in ^{40}Ca . Since the Q value for the (n, γ) reaction is 7.80 MeV and the first $T = 1$ level in ^{40}Ca occurs at $E_x = 7.64$ MeV, D is initially obtained at $E_x \approx 15.5$ MeV in ^{40}Ca . The assumption is made that the resonances observed in the $^{39}\text{K}(n, \gamma)^{40}\text{K}$ reaction are formed by S -wave capture only, and therefore must have $J^\pi = 1^+$ or 2^+ . The spacing of $J^\pi = 1^-$ levels can then be deduced from the experimental data using the following two general predictions¹⁸ of statistical models of nuclear level densities: (1) Positive- and negative-parity compound-nucleus levels occur with equal probability, and (2) the density of levels of a given (small) J is weighted by $2J + 1$. The result is $D = 14.8$ keV for $J^\pi = 1^-$, $T = 1$ levels at $E_x = 15.5$ MeV in ^{40}Ca . The extrapolation to 19 MeV is then made using the level-density formula given by Preston¹⁹ which, for small J is

$$\rho(E, J) = (2J + 1) \frac{18.5 \alpha A^{1/2}}{(E + t)^2 A^{5/2}} e^{2\sqrt{\alpha E}}, \quad (2)$$

where t is the nuclear temperature, A is the mass number, and the value $\alpha = 6.0$ is suggested by Preston. The parameter a is, in general, ex-

pected^{20, 21} to lie between $A/10$ and $A/7.4$, and is chosen here as $a = 4.47 \approx A/9$ in order to give agreement between D and (2) at $E_x = 15.5$ MeV. Finally, one obtains $D = 3.1$ keV at $E_x = 19$ MeV in ^{40}Ca and, therefore, $\Gamma/D \approx 8$. Using (2) to calculate D as a function of energy and estimating Γ from arguments based on penetrability factors and the fact that the neutron channel just opens at 15.61 MeV, it can be shown that $\Gamma/D \approx 1$ down to $E_x \approx 16$ MeV. Hence, in the following, the fine structure observed in the 90° excitation function in the range $16 \text{ MeV} \leq E_x \leq 23 \text{ MeV}$ will be treated in terms of Ericson's theory.

Considering first the case of a reaction which proceeds via compound-nucleus formation with amplitude $f(E)$ and via an energy-independent "direct" process with amplitude d , the cross section $\sigma(E)$ is given by

$$\sigma(E) = |d + f(E)|^2. \quad (3)$$

Denoting averages over energy by $\langle \rangle$, and with the definitions

$$\sigma_D = |d|^2 \quad (4)$$

and

$$\langle \sigma_{CN} \rangle = \langle |f(E)|^2 \rangle \quad (5)$$

it can be shown that

$$\langle \sigma \rangle = \sigma_D + \langle \sigma_{CN} \rangle. \quad (6)$$

The two processes contribute coherently to the cross section at a given energy but incoherently to the average cross section. Using Ericson's definition of the autocorrelation function $R(\epsilon)$,

$$R(\epsilon) = \frac{\langle \sigma(E)\sigma(E+\epsilon) \rangle}{\langle \sigma \rangle^2} - 1, \quad (7)$$

one obtains the following relation between $R(\epsilon)$, Γ , and σ_D for a reaction in which one channel dominates,

$$R(\epsilon) = (1 - Y_D^2) \frac{1}{1 + (\epsilon/\Gamma)^2}, \quad (8)$$

where

$$Y_D = \sigma_D / \langle \sigma \rangle. \quad (9)$$

As can be seen from Eq. (8), $R(\epsilon)$ has a Lorentzian shape with half width at half maximum equal to Γ .

In the present case of the $^{39}\text{K}(p, \gamma_0)^{40}\text{Ca}$ reaction in the GDR, it can be deduced from the energy independence of the angular distributions that only one independent channel contributes, assuming that it is unlikely that two independent channels will combine to generate the same angular distribution at all energies. However, the amplitude d in Eq. (3) can no longer be taken as energy-independent. Allardyce *et al.*²² have shown that if $d(E)$

TABLE II. Resonance parameters for giant-dipole-resonance peaks in ^{40}Ca .

	Lower peak	Upper peak
$\sigma_0(\gamma, p_0)$ (mb/sr)	1.95 ± 0.1	0.35 ± 0.25
Γ (MeV)	3.1 ± 0.2	3.2 ± 0.5
E_x (MeV)	19.3 ± 0.1	22.0 ± 0.5
% of dipole strength	84 ± 13	16 ± 12

varies smoothly with energy, then $R(\epsilon)$ defined by Eq. (7) retains a Lorentzian shape but is shifted up from the ϵ axis by a function $K(\epsilon)$ -dependent both in magnitude and form on $d(E)$. Various methods for removing the $K(\epsilon)$ modulation from $R(\epsilon)$ have been suggested^{2, 21-26}; two, referred to as the difference technique and the moving average technique, will be employed here.

In the difference technique,²³ two autocorrelation functions $R_1(\epsilon)$ and $R_2(\epsilon)$ are calculated from the data. $R_1(\epsilon)$ is computed according to Eq. (7). $R_2(\epsilon)$ is computed from the definition

$$R_2(\epsilon) = \frac{\langle \sigma(E)\sigma(E+\epsilon) \rangle_{av} - 1}{\langle \sigma \rangle^2}, \quad (10)$$

where the notation $\langle \sigma(E) \rangle_{av}$ indicates an average over an energy interval large in comparison to the fine structure but significantly smaller than the energy range of the data. Defining $R_\Delta(\epsilon)$ by

$$R_\Delta(\epsilon) = R_1(\epsilon) - R_2(\epsilon) \quad (11)$$

one obtains Γ and Y_D from Eq. (8), with $R_\Delta(\epsilon)$ replacing $R(\epsilon)$.

In the moving average technique,^{2, 25} the autocorrelation function is defined by

$$R(\epsilon) = \left(\frac{\sigma(E)}{\langle \sigma(E) \rangle_q} - 1 \right) \left(\frac{\sigma(E+\epsilon)}{\langle \sigma(E+\epsilon) \rangle_q} - 1 \right). \quad (12)$$

The notation $\langle \sigma(E) \rangle_q$ indicates an average over an energy interval $q = 2\delta E$ extending from $E - \delta E$ to $E + \delta E$. The value of q to be used in the calculation of $R(\epsilon)$ is determined by computing $R(0)$ as a function of q . For $q=0$, $R(0)=0$. As q increases, $R(0)$ also increases, until the averaging interval is large enough to average out the narrowest structure. $R(0)$ then levels off and is independent

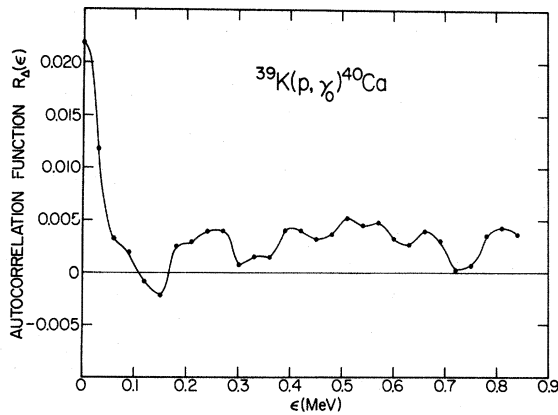


FIG. 6. Autocorrelation function $R(\epsilon)$ between the $^{39}\text{K}(p, \gamma_0)^{40}\text{Ca}$ cross section observed at E and at $E + \epsilon$, computed with the difference technique (see text). E extends from 16 to 23 MeV.

of q provided q is significantly less than the width of any other structure which might be present. $R(\epsilon)$ is then calculated for q within this "plateau" region of $R(0)$. Values of Γ and Y_D are deduced from $R(\epsilon)$ according to the relation given by Eq. (8).

The autocorrelation functions were calculated by the two techniques discussed above using the data of Fig. 2 in the range $16 \text{ MeV} \leq E_x \leq 23 \text{ MeV}$. $R_\Delta(\epsilon)$ obtained in the difference technique with a 200-keV averaging interval used for the calculation of $R_2(\epsilon)$, is shown in Fig. 6. The 200-keV averaging interval was chosen to remove from $R_\Delta(\epsilon)$ effects of intermediate structure and the GDR envelope. The resulting coherence width, after correction for target thickness and the finite energy range of the data, is $14 \text{ keV} \pm 12 \text{ keV}$. This is in agreement with the previously noted results of a fine-structure analysis of the $^{39}\text{K}(p, \alpha)^{36}\text{Ar}$ reaction.¹¹ It is, however, smaller than the estimate $\Gamma \approx 25 \text{ keV}$ made from Fig. 2, although the two are compatible within the large error which comes mainly from uncertainty in the target thickness. From the value $R(0) = 0.022$, one concludes that only $\sim 1\%$ of the average (p, γ_0) cross section results from the fluctuating compound-nucleus processes. For comparison, in ^{28}Si , the corresponding number¹⁰ is $\sim 4\%$.

Using the moving average technique, the dependence of $R(0)$ [Eq. (12)] on the averaging interval q was determined and is shown in the inset of Fig. 7. Changes in slope are evident at $q \approx 350 \text{ keV}$ and $q \approx 700 \text{ keV}$. The first corresponds to an averaging interval for which all weak intermediate-structure peaks have been averaged out, as

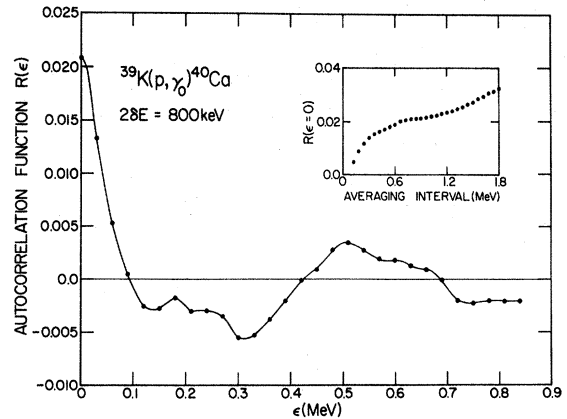


FIG. 7. Autocorrelation function $R(\epsilon)$ between the $^{39}\text{K}(p, \gamma_0)^{40}\text{Ca}$ cross section at E and $E + \epsilon$, obtained from the moving average technique (see text) with an 800-keV averaging interval. The inset shows $R(\epsilon)$ for $\epsilon = 0$ as a function of the averaging-interval width.

can be seen in Fig. 2. $R(0)$ is still sensitive to q , however, since the width of the intermediate-structure peaks is approximately equal to q . No plateau develops for $R(0)$ until q is large enough to average out the intermediate structure also, which occurs at $q \approx 700$ keV. Here a relatively flat region develops for q between 750 and 930 keV. The subsequent increase in $R(0)$ as q becomes still larger is attributable to the envelope of the GDR. The autocorrelation function $R(\epsilon)$ shown in Fig. 7 was calculated with $q = 800$ keV. The coherence width $\Gamma = (26 \pm 13)$ keV is obtained, which is in agreement with the estimate $\Gamma \approx 25$ keV made from Fig. 2 and, within the large error, with the result derived above in the difference technique. The two methods yield essentially the same number for $R(0)$, which is considered somewhat fortuitous since different averaging intervals were used. For averaging intervals up to 1.0 MeV, however, both methods indicate that <3% of the average $^{39}\text{K}(p, \gamma_0)^{40}\text{Ca}$ cross section is the result of compound-nucleus processes.

The variation of Γ as a function of excitation energy was investigated using the moving average technique and 2-MeV sections of the excitation function, with q again equal to 800 keV. A monotonic increase from $\Gamma = 22$ keV for $16 \text{ MeV} \leq E_x \leq 18 \text{ MeV}$ to $\Gamma = 32$ keV for $20 \text{ MeV} \leq E_x \leq 22 \text{ MeV}$ was obtained which, although within experimental and statistical uncertainties, may indicate the growing contribution of the neutron channel to the width of the compound-nucleus levels.

The small percentage obtained for the compound-nucleus contribution to the (p, γ_0) cross section in the GDR is consistent with the assumption that the fine structure is caused by weak compound-nucleus states interfering with the dominant giant dipole state.²⁷ Fluctuations in the cross section are then expected to be of greatest magnitude near the peak of the GDR. This feature is clearly observed in Fig. 2. The fact that the angular distributions are approximately energy-independent can also be explained. Capture of the incoming proton initially sets up the coherent giant dipole state, which then decays by γ emission or proceeds to more-complicated (less coherent) configurations. Thus, the angular distributions are determined mainly by the giant dipole (doorway) state.

V. INTERMEDIATE STRUCTURE

Table I lists the energies of the intermediate-structure peaks taken from the 100-keV averaged data of Fig. 5. Corresponding peaks have been observed in the excitation functions of the reactions $^{40}\text{Ca}(\gamma, p_0)$, $^{40}\text{Ca}(\gamma, n_0)$; $^{40}\text{Ca}(\gamma, n)^{12}$; and

$^{39}\text{K}(p, \alpha_0)$, $^{39}\text{K}(p, \alpha_1)$, $^{39}\text{K}(p, p_0)$, and $^{39}\text{K}(p, p')$ for several inelastic channels.^{28, 29} Various proposals have been advanced to explain intermediate structure and can be separated into two broad groupings: statistical fluctuations due to overlapping levels^{16, 30} and resonance structure caused by individual levels.³¹⁻³³

In the former category, Singh, Hoffman-Pinter, and Lang³⁰ and others have shown that in a given reaction channel a random "lumping" of compound-reaction amplitudes can produce structure of width greater than Γ_{CN} , i.e., the average width of the compound levels. However, the correlation between cross sections for different channels should be zero when calculated for a statistically meaningful energy interval, unless the symmetry of the interaction with respect to the two channels implies the same amplitudes [e.g. the (γ, p_0) and (γ, n_0) excitation functions should be similar⁶ to the degree to which Coulomb effects can be ignored]. The correlation between the various particle channels²⁹ seems to rule out this explanation.

In the latter grouping, Moldauer³¹ had proposed a statistical theory of intermediate structure which for strongly absorptive incident channels predicts individual resonances which may appear at the same excitation energy in various exit channels. These resonances are expected to exhibit a broad range of widths, but the intermediate peaks observed here are clustered in a range of a few 100 keV as is illustrated by the two bends in the autocorrelation function in the insert of Fig. 7. A likely interpretation of the observed intermediate structure is that in terms of more complicated states which are coupled to the 1p-1h collective doorway state.³² A calculation including 3p-3h states has recently been done³³ in ^{16}O and resulted in good agreement with the experiment.

VI. DESCRIPTION OF THE GDR

The gross structure of the excitation function of Fig. 2 indicates two wide peaks (with characteristics listed in Table II), which are now identified with the 1p-1h dipole states and are compared in Fig. 8 to the various theoretical predictions.

Gillet and Sanderson computed the negative-parity states in ^{40}Ca both by diagonalizing the particle-hole interaction³⁴ and by the random-phase approximation.³⁵ The residual interaction employed was a central potential with Gaussian radial dependence and exchange terms. Nearly all single-particle and hole energies were taken from experimental data. Coulomb effects were taken into account by reducing the proton particle-hole energy by 0.66 MeV³⁴ (0.5 MeV)³⁵ for diagonal matrix elements of the residual interaction. Us-

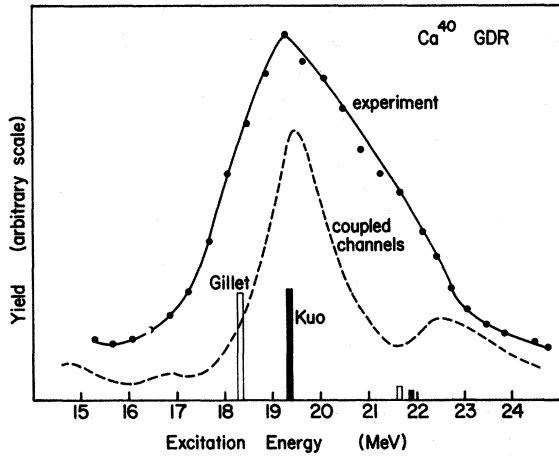


FIG. 8. Comparison of the averaged $^{39}\text{K}(p, \gamma)^{40}\text{Ca}$ yield function with various theoretical predictions for the electric-dipole strength distribution in ^{40}Ca . The bound-state results of Gillet (Ref. 35) and Kuo (Ref. 3) as well as the continuum calculations for the (p, γ_0) cross section of Ref. 4 are indicated.

ing the single-particle wave functions of an infinite harmonic-oscillator well, the calculations predicted 90% of the $E1$ strength in one state located between 18.3 MeV³⁴ and 18.76 MeV.³⁵ A state ~ 3 MeV higher contained the remaining 10% of the $E1$ strength. Comparison with experiment shows that the predicted energy of the GDR is about 1 MeV too low. The disagreement between the experimental and theoretical GDR energies was attributed³⁴ in part to the use of too small a value for the energy of the $d_{5/2}$ hole, namely, 5.9 MeV. In the calculation of Ref. 35, this energy was taken as 6.4 MeV, but the GDR was still predicted ~ 0.5 MeV too low.

The $d_{3/2}$ hole components are of special interest in the present work since, in the shell model, the ^{39}K ground state is just a $d_{3/2}$ proton hole in ^{40}Ca . The predicted amplitudes of the $f_{5/2}d_{3/2}^{-1}$, $p_{3/2}d_{3/2}^{-1}$, and $p_{1/2}d_{3/2}^{-1}$ configurations in the giant dipole state are 0.50, 0.04, and 0.12, respectively. (These are in general agreement with expectations based on the simple schematic model.³⁶) The state at higher energy contains appreciably only the $f_{5/2}d_{5/2}^{-1}$ and $f_{5/2}d_{3/2}^{-1}$ configurations with coefficients 0.95 and 0.25, respectively.

Direct comparison of the bound-state calculations with the experimental cross sections and angular distributions cannot quantitatively be made. It is noted, though, that the experimentally observed $A_2 = -0.33$ is consistent with dominant f -wave capture (for pure f -wave capture, one would observe $A_2 = -0.40$). The large ratio for the $(f_{5/2}d_{3/2}^{-1})$ to $(p_{1/2}d_{3/2}^{-1})$ amplitudes in the giant di-

pole state is therefore in qualitative agreement with the experiment.

Blomquist and Kuo³ calculated the negative-parity one-particle-one-hole states in ^{40}Ca using the Hamada-Johnston potential, single-particle wave functions of an infinite harmonic-oscillator well, and the random-phase approximation. The effect of core polarization was also investigated. Essentially the same single-particle and hole energies were used as given by Gillet and Sanderson.³⁴ Coulomb effects were included in diagonal matrix elements, but with a reduced correction of 0.32 MeV. The resulting wave functions exhibit 1p-1h amplitudes comparable to those obtained previously, but the predicted energies for the main GDR are closer to the experimentally observed value. In fact, in the calculation of Blomquist and Kuo, which gives the best agreement with experimentally determined energies of 3^- and 5^- states at low excitation energies, a giant dipole state with 93% of the $E1$ strength is obtained at 19.53 MeV to be compared with the presently observed 19.3 ± 0.1 MeV. An additional state at 22.10 MeV containing 7% of the sum rule is also in accord with the experiment.

The coupled-channel theory¹ was applied to ^{40}Ca by Marangoni and Saruis.⁴ A real Woods-Saxon well with spin-orbit and Coulomb terms was employed for the single-particle potential with well parameters adjusted to reproduce the single-particle energies of Gillet and Sanderson.³⁴ A zero-range residual force was assumed and residual Coulomb interaction effects included. These calculations yield directly the $\sigma(\gamma, p_0)$ cross section. Resonances containing appreciable dipole strength are predicted at 19.5 and 22.4 MeV, with peak (γ, p_0) cross sections³⁷ of 200 and 28 mb, respectively. Experimental peak total cross sections obtained in the present work are 21 mb at the 19.3-MeV resonance and 3.8 mb at the 22-MeV resonance. Although the energies agree well, the predicted cross sections are about 10 times larger than the experimentally obtained values. The predicted widths of approximately 1 MeV for the two states are only one third of the experimental widths. The disagreement between the predicted and observed cross sections and widths is at least partially attributable to exclusion of an absorptive potential from the (γ, p_0) calculation. The (γ, p) cross section was calculated⁴ both with and without an absorptive potential $W(E) = 0.05E(\text{MeV}) = 0.5$. The widths are increased to 1.5 MeV with the inclusion of the absorptive potential, and the peak total (γ, p) cross section at 19.5 MeV is reduced from ~ 465 mb ($W = 0$) to ~ 120 mb. As discussed above, the present work indicates that $\sim 25\%$ of the (γ, p) strength goes into the p_0 channel.

The predicted (γ, p_0) peak cross section then becomes 30 mb, close to the observed value of 21 mb. The total width, however, is still less than the observed value.

The coupled-channels calculations also yield angular distributions for the $^{39}\text{K}(p, \gamma_0)^{40}\text{Ca}$ reaction, and the predicted A_2 coefficients are compared to experiment in Fig. 4. Between 18 and 21 MeV the signs agree but the predicted average value $A_2 = -0.12$ is consistently only about $\frac{1}{2}$ of

what is observed. Above 21 MeV the predicted A_2 becomes positive with +0.34 at ~ 21.5 MeV, at variance with experiment.

In summary, it appears that in ^{40}Ca the 1p-1h calculations predict accurately the energies and approximate dipole strength distributions. However, the coupled-channels continuum calculations fail, as in earlier cases, to give the correct widths and angular distribution.

†Work supported by the National Science Foundation.

*Present address: Department of Physics, Stanford University, Stanford, California.

‡A. P. Sloan Foundation Fellow.

¹B. Buck and A. D. Hill, Nucl. Phys. **A95**, 271 (1967).

²J. E. E. Bablin and M. N. Thompson, Nucl. Phys. **A158**, 73 (1969), and references therein.

³J. Blomqvist and T. T. S. Kuo, Phys. Letters **29**, 649 (1969).

⁴M. Marangoni and A. M. Sarius, Nucl. Phys. **A132**, 649 (1969).

⁵J. C. Hafele, F. W. Bingham, and J. S. Allen, Phys. Rev. **164**, 1397 (1967).

⁶C. P. Wu, J. E. E. Baglin, F. W. K. Firk, and T. W. Phillips, Phys. Letters **29B**, 359 (1969).

⁷E. M. Diener, J. F. Amann, S. L. Blatt, and P. Paul, Nucl. Instr. Methods **83**, 115 (1970).

⁸J. Bartko and T. T. Thwaites, Phys. Letters **27B**, 212 (1968).

⁹F. S. Dietrich, M. Suffert, A. V. Nero, and S. S. Hanna, Phys. Rev. **168**, 1169 (1968).

¹⁰P. P. Singh, R. E. Segel, L. Meyer-Schutzmeister, S. S. Hanna, and R. G. Allas, Nucl. Phys. **65**, 577 (1965).

¹¹D. von Ehrenstein, L. Meyer-Schutzmeister, and R. G. Allas, Nucl. Phys. **79**, 625 (1966).

¹²J. M. Wyckoff, B. Ziegler, H. W. Koch, and R. Uhling, Phys. Rev. **137**, B576 (1965).

¹³J. E. E. Baglin and B. M. Spicer, Nucl. Phys. **54**, 549 (1964).

¹⁴N. W. Tanner, G. C. Thomas, and E. D. Earle, Nucl. Phys. **52**, 29 (1964).

¹⁵M. Danos and W. Greiner, Phys. Rev. **138**, B876 (1965).

¹⁶T. Ericson, Ann. Phys. (N.Y.) **23**, 390 (1963).

¹⁷A. Moldauer, Phys. Letters **8**, 70 (1964).

¹⁸T. Ericson, Advan. Phys. **9**, 425 (1960).

¹⁹M. A. Preston, *Physics of the Nucleus* (Addison-Wesley, Reading, Massachusetts, 1962), p. 527.

²⁰H. K. Vonach, A. A. Katsanos, and J. R. Huizenga, Nucl. Phys. **A122**, 465 (1968).

²¹P. J. Dallimore and B. W. Allardyce, Nucl. Phys. **A108**, 150 (1968).

²²B. W. Allardyce, P. J. Dallimore, I. Hall, N. W. Tanner, A. Richter, P. von Brentano, and T. Mayer-Kuchuk, Nucl. Phys. **85**, 193 (1966).

²³R. C. Barse, L. Meyer-Schutzmeister, and R. E. Segel, Nucl. Phys. **A116**, 682 (1968).

²⁴E. Gadioli, I. Iori, and A. Marini, Nuovo Cimento **39**, 996 (1965).

²⁵G. Pappalardo, Phys. Letters **13**, 320 (1964).

²⁶C. M. Lamba, N. Sarma, N. S. Thampi, D. K. Sood, and V. K. Deshpande, Nucl. Phys. **A110**, 111 (1968).

²⁷N. W. Tanner, Nucl. Phys. **63**, 383 (1965).

²⁸H. Feshbach, in *Proceedings of the International Conference on Nuclear Physics, Gatlinburg, Tennessee, 12-17 September 1966*, edited by R. L. Becker, C. D. Goodman, P. H. Stelson, and A. Zucker (Academic, New York, 1967), p. 188.

²⁹G. J. F. Legge and M. S. Krick, in *Contributions, International Conference on Properties of Nuclear States, Montreal, Canada, 1969* (Presses de l'Université de Montréal, Montréal, Canada, 1969), p. 360.

³⁰P. P. Singh, P. Hoffman-Pinter, and D. W. Lang, Phys. Letters **23**, 255 (1966).

³¹P. A. Moldauer, Phys. Rev. Letters **18**, 249 (1967).

³²H. Feshbach, A. K. Kerman, and R. H. Lemmer, Ann. Phys. (N.Y.) **41**, 230 (1967).

³³C. M. Shakin and W. L. Wang, Phys. Rev. Letters **26**, 902 (1971); W. L. Wang and C. M. Shakin, Phys. Rev. **C 5**, 1898 (1972).

³⁴V. Gillet and E. A. Sanderson, Nucl. Phys. **A91**, 472 (1967).

³⁵V. Gillet and E. A. Sanderson, Nucl. Phys. **A91**, 292 (1967).

³⁶G. E. Brown, *Unified Theory of Nuclear Models and Forces* (North-Holland, Amsterdam, 1967), p. 29.

³⁷C. Mahaux and A. M. Sarius, Nucl. Phys. **A138**, 481 (1969).